

Optoelectronic properties of single-crystalline GaInAsSb quaternary alloy nanowires

Meng-Zi Li(李梦姿), Xin-Liang Chen(陈新亮), Hong-Lai Li(李洪来), Xue-Hong Zhang(张学红), Zhao-Yang Qi(祁朝阳), Xiao-Xia Wang(王晓霞), Peng Fan(范鹏), Qing-Lin Zhang(张清林), Xiao-Li Zhu(朱小莉), Xiu-Juan Zhuang(庄秀娟)

Citation: Chin. Phys. B . 2018, 27(7): 078101. **doi:** 10.1088/1674-1056/27/7/078101

Journal homepage: http://cpb.iphy.ac.cn; http://iopscience.iop.org/cpb

What follows is a list of articles you may be interested in

High performance photodetectors based on high quality InP nanowires

Yan-Kun Yang(杨燕琨), Tie-Feng Yang(杨铁锋), Hong-Lai Li(李洪来), Zhao-Yang Qi(祁朝阳), Xin-Liang Chen(陈新亮), Wen-Qiang Wu(吴文强), Xue-Lu Hu(胡学鹿), Peng-Bin He(贺鹏斌), Ying Jiang(蒋英), Wei Hu(胡伟), Qing-Lin Zhang(张清林), Xiu-Juan Zhuang(庄秀娟), Xiao-Li Zhu(朱小莉), An-Lian Pan(潘安练)

Chin. Phys. B . 2016, 25(11): 118106. **doi:** 10.1088/1674-1056/25/11/118106

Preparation of patterned boron nanowire films with different widths of unit-cell and their field emission properties

Yong-Xin Zhang(张永欣), Fei Liu(刘飞), Cheng-Min Shen(申承民), Jun Li(李军), Shao-Zhi Deng(邓少芝), Ning-Sheng Xu(许宁生), Hong-Jun Gao(高鸿钧)

Chin. Phys. B . 2016, 25(8): 088102. **doi:** 10.1088/1674-1056/25/8/088102

Preparation of few-layer graphene-capped boron nanowires and their field emission properties

Yong-Xin Zhang(张永欣), Fei Liu(刘飞), Cheng-Min Shen(申承民), Tian-Zhong Yang(杨天中), Jun Li(李军), Shao-Zhi Deng(邓少芝), Ning-Sheng Xu(许宁生), Hong-Jun Gao(高鸿钧)

Chin. Phys. B . 2016, 25(7): 078101. **doi:** 10.1088/1674-1056/25/7/078101

Electronic transport properties of silicon junctionless nanowire transistors fabricated by femtosecond laser direct writing

Liu-Hong Ma(马刘红), Wei-Hua Han(韩伟华), Hao Wang(王昊), Qi-feng Lyu(吕奇峰), Wang Zhang(张望), Xiang Yang(杨香), Fu-Hua Yang(杨富华)

Chin. Phys. B . 2016, 25(6): 068103. **doi:** 10.1088/1674-1056/25/6/068103

Charge trapping in surface accumulation layer of heavily doped junctionless nanowire transistors

Ma Liu-Hong, Han Wei-Hua, Wang Hao, Yang Xiang, Yang Fu-Hua

Chin. Phys. B . 2015, 24(12): 128101. **doi:** 10.1088/1674-1056/24/12/128101

Optoelectronic properties of single-crystalline GaInAsSb quaternary alloy nanowires*

Meng-Zi Li(李梦姿), Xin-Liang Chen(陈新亮), Hong-Lai Li(李洪来), Xue-Hong Zhang(张学红), Zhao-Yang Qi(祁朝阳), Xiao-Xia Wang(王晓霞), Peng Fan(范鹏), Qing-Lin Zhang(张清林), Xiao-Li Zhu(朱小莉)†, and Xiu-Juan Zhuang(庄秀娟)‡

Key Laboratory for Micro-Nano Physics and Technology of Hunan Province, School of Physics and Electronic Science, Hunan University, Changsha 410082, *China*

(Received 27 December 2017; revised manuscript received 11 April 2018; published online 25 June 2018)

Bandgap engineering of semiconductor nanomaterials is critical for their applications in nanoelectronics, optoelectronics, and photonics. Here we report, for the first time, the growth of single-crystalline quaternary alloyed $Ga_{0.75}In_{0.25}As_{0.49}Sb_{0.51}$ nanowires via a chemical-vapor-deposition method. The synthesized nanowires have a uniform composition distribution along the growth direction, with a zinc-blende structure. In the photoluminescence investigation, these quaternary alloyed semiconductor nanowires show a strong band edge light emission at 1950 nm (0.636 eV). Photodetectors based on these alloy nanowires show a strong light response in the near-infrared region (980 nm) with the external quantum efficiency of 2.0×10^4% and the responsivity of 158 A/W. These novel near-infrared photodetectors may find promising applications in integrated infrared photodetection, information communication, and processing.

Keywords: GaInAsSb nanowire, quaternary alloy, near-infrared photodetector

PACS: 81.07.Gf, 74.70.Dd, 85.60.Gz **DOI:** 10.1088/1674-1056/27/7/078101

1. Introduction

One-dimensional semiconductor nanowires have attracted considerable attention as unique building blocks for various applications in integrated electronic and optoelectronic devices, such as nanoscale lasers,[1–3] field effect transistors,[4–6] solar cells,[7] and photodetectors (PDs).[8,9] Nanowire-based PDs, as potential key functional units in on-chip information communication and processing, have attracted considerable interest.[10–12] Particularly, PDs constructed by III–V semiconductor nanowires are widely used in near-infrared and infrared detection due to their narrow bandgap.[13,14] Compared to the binary III–V semiconductor nanowires, the alloyed III–V semiconductor wires usually have wider and adjustable spectral response ranges due to their tunable bandgap nature, which means that the III–V alloy nanowires are ideal systems that are promising candidates for constructing wide-spectral-response-range and high-performance PDs in the infrared region.[15–21] Among the many III–V alloys, $Ga_{1-x}In_xAs_ySb_{1-y}$ is an important quaternary alloy with tunable bandgap from 1.42 eV ($x = 0$, $y = 1$) to 0.1 eV ($x = 1$, $y = 0$), this widely tunable bandgap range covers three important spectral regions 1–3 μm, 3–5 μm, and 8–14 μm.[22] So far, GaInAsSb layers based PDs have been successfully constructed,[23,24] however, the photoelectric measurement based on quaternary GaInAsSb alloy nanowires is rarely reported in the literature.

Quaternary $Ga_{1-x}In_xAs_ySb_{1-y}$ alloys have usually been grown by liquid phase epitaxy (LPE),[25] organometallic vapor phase epitaxy (MOVPE),[26] molecular beam epitaxy (MBE),[27] and metal-organic chemical-vapor-deposition (MOCVD).[28] For the preparation of GaInAsSb quaternary alloy nanowires, there is a challenge to obtain the GaInAsSb nanowires with compositions in the miscibility gap through LPE or other thermodynamic equilibrium methods. Although, the non-equilibrium growth techniques, such as MBE and MOCVD, can effectively overcome this difficulty, the above growth strategies usually have a high cost and the preparation process is complicated. To the best of our knowledge, there is no report on the GaInAsSb alloy nanowires synthesized via a chemical vapor deposition (CVD) method, which is a cheaper method and easy to operate.

In this work, high-quality GaInAsSb quaternary alloyed nanowires were synthesized via a simple CVD method. Both Raman spectrum and photoluminescence studies show bandgap engineered optical properties consistent with the composition of the alloy nanowires. Single-nanowire-PDs with high responsivity and external quantum efficiency in the near-infrared region were constructed. Our results of these novel PDs will advance the development of photonics and optoelectronics as well as the integrated devices.

*Project supported by the National Natural Science Foundation of China (Grant Nos. 51525202, 61505051, 1137049, 61474040, and 61635001), the Aid Program for Science and Technology Innovative Research Team in Higher Educational Institutions of Hunan Province, China, and the Fundamental Research Funds for the Central Universities, China.

†Corresponding author. E-mail: zhuxiaoli@hnu.edu.cn

‡Corresponding author. E-mail: zhuangxj@hnu.edu.cn

© 2018 Chinese Physical Society and IOP Publishing Ltd

2. Experiments

The samples were grown in a horizontal furnace, where a moving source method was applied for the composition modulation.[29] Typically, an alumina boat with GaSb powder (Aladdin, 99.99%) was firstly pulled into the heating zone of the furnace, and another boat with InAs powder (Aladdin, 99.99%) was placed far away from the heating zone. A quartz rod driven by a step motor through magnetic force was used to push the boats into or out of the heating zone during the growth. Silicon wafers coated with 5-nm-thick gold film were placed in the deposition area to collect the samples. Before heating, mixed gas (Ar with 5% H_2) was flowed into the system at a rate of 45 sccm and the pressure was maintained at 4 Torr. Then the furnace was heated to 750 °C at a rate of 30 °C·min^{-1}. After 60 min of growth at 750 °C, the InAs powder was shifted to the center of the heating zone slowly. After keeping on the growth for another 60 min, the furnace was naturally cooled to room temperature.

The morphology and structure of the as-prepared sample were characterized by a field emission scanning electron microscope (FE-SEM, Zeiss sigma-HD), an x-ray diffraction spectrometer (XRD, Rigaku D/Max 2500), and a transmissionelectron microscope (TEM, Tecai F20) combined with energy-dispersive x-ray spectroscopy (EDX). The Raman scattering spectra were collected on a laser confocal Raman spectrometer (LABRAM-010, France), while PL measurements were conducted via a home-built infrared micro-PL setup with a femtosecond laser excitation source (Spectra Physics Tsunami, 800 nm, 80 fs pulse duration, 80 MHz repetition rate).

PDs were constructed with the as-prepared single $Ga_{0.75}In_{0.25}As_{0.49}Sb_{0.51}$ nanowires. The nanowires were first dispersed on a p-type Si substrate with a 300 nm thickness SiO_2 layer. Then AMMA and PMMA were spin-coated on the surface of the mask. The electron-beam lithography system (RAITH: 150-TWO) was employed to design the electrode patterns. Two Cr/Au (10/60 nm) electrodes that acted as the source and drain were fabricated by a thermally deposited process. The single nanowire connected with the Cr/Au Schottky contact electrodes constitutes a typical M-S-M PD. The as-fabricated PDs were investigated by a semiconductor parameter analyzer (Keithley 4200) under dark conditions and the illumination of a monochromatic light beam, all the measurements were carried out at room temperature.

3. Result and discussion

The SEM image of the as-grown sample (Fig. 1(a)) shows that the synthesized nanowires have a length of up to 10 μm and a diameter ranging between 150 nm and 300 nm. The inset of Fig. 1(a) shows a high-magnification SEM image of a typical nanowire. Figure 1(b) exhibits the XRD pattern of the as-deposited quaternary alloy nanowires. For comparison, we list the standard XRD patterns of zinc-blende (ZB) GaAs (JCPDS card No. 89-2770; $a = 5.65330$ Å) and ZB InSb (JCPDS card No. 70-2515; $a = 6.47937$ Å) in the top and bottom of the graph, respectively. The sharp diffraction peaks indicate that the as-grown nanowires are GaInAsSb alloy with pure ZB crystallographic phase and high phase purity.

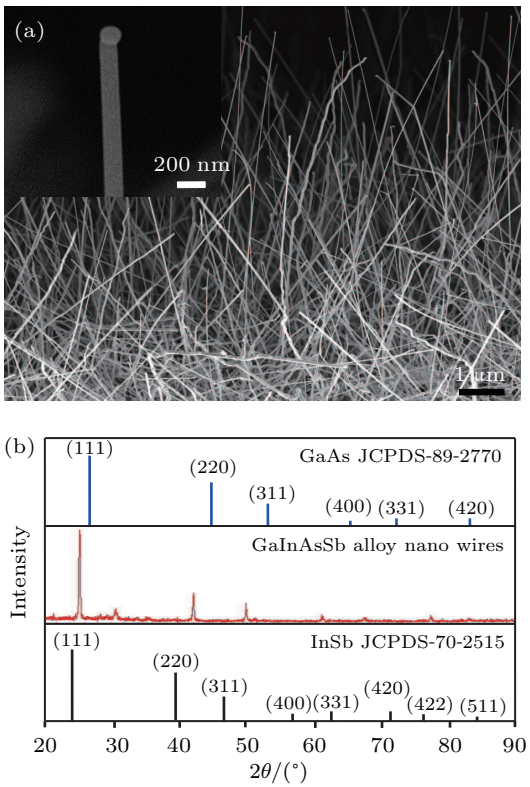


Fig. 1. (color online) (a) SEM image of the as-grown nanowires. Inset: high-resolution SEM image of a single nanowire with catalyst. (b) The XRD pattern of the as-deposited alloy nanowires.

Figure 2(a) is the TEM image of a representative nanowire. There is a typical spherical catalytic particle at the tip of the nanowire, which demonstrates that the growth of these nanowires follows the typical metal-catalyzed vapour–liquid–solid (VLS) mechanism.[30] Figure 2(b) shows the high-resolution TEM (HRTEM) image taken from the nanowire (the red rectangle in Fig. 2(a)). The d-spacing of (220) planes was measured to be 0.2124 nm, falling in between the values of GaAs and InSb (Cf. $d_{GaAs} = 1.9988$ Å and $d_{InSb} = 2.2907$ Å). The insert of Fig. 2(b) plots the corresponding reciprocal lattice space image extracted by fast-Fourier transform (FFT) along the $[1\bar{1}0]_{ZB}$ zone axes. According to the FFT patterns, the crystal structure of the nanowire can be confirmed to be the ZB structure, and their growth direction is [110]. Meanwhile, the clear and orderly atomic arrangement further reveals that the nanowire has a high-quality single-crystalline structure without significant stacking faults or twin-plane polytypic defects. Figure 2(c) plots

the EDS spectrum collected from the wire (the red dot in the inset of the figure), which illustrates that the nanowire consists of elements Ga, In, As, and Sb with the ratio of 0.75:0.25:0.49:0.51, revealing that the composition of the achieved wires is $Ga_{0.75}In_{0.25}As_{0.49}Sb_{0.51}$. Figure 2(d) displays the two-dimentional (2D) elemental mapping of this nanowire, indicating that Ga, In, As, and Sb are homogeneously distributed across the whole nanowire.

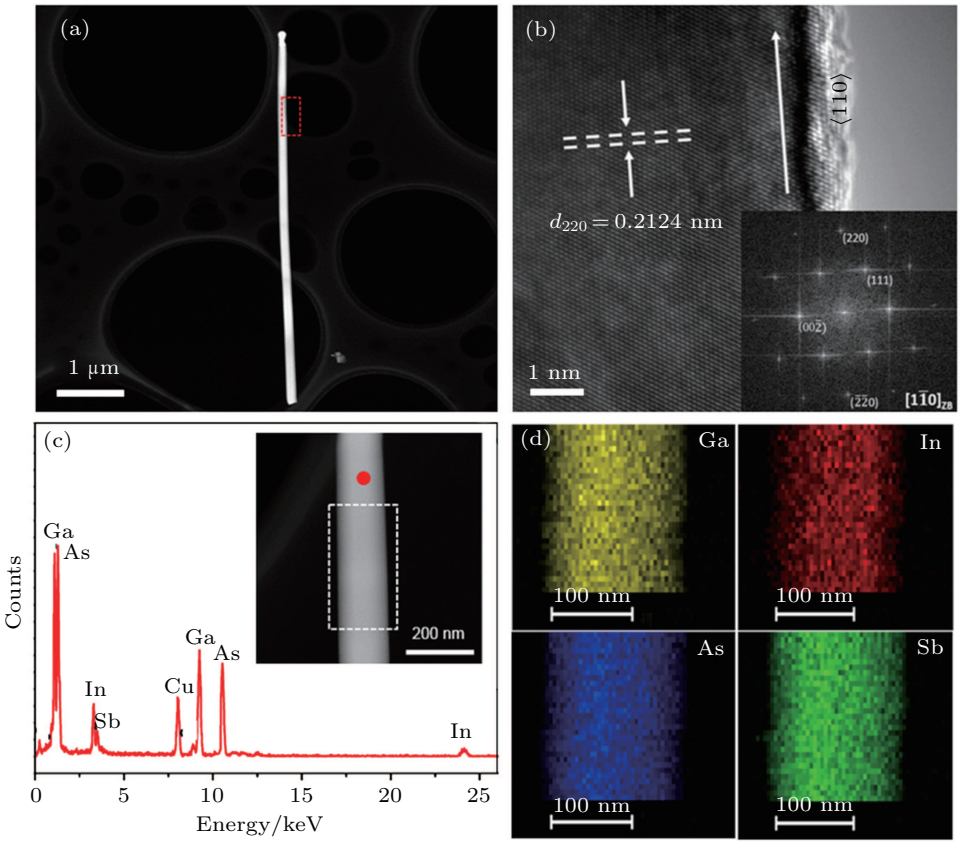


Fig. 2. (color online) (a) TEM image of a representative single GaInAsSb nanowire. (b) HRTEM image taken from the red rectangle of (a), the insert is the diffraction pattern converted by fast-Fourier transform where the zone axis $[1\bar{1}0]_{ZB}$ can be identified. (c) Corresponding EDX profiles measured at the red dot of the nanowire. (d) The 2D elemental mapping of the four detected elements Ga, In, As, and Sb.

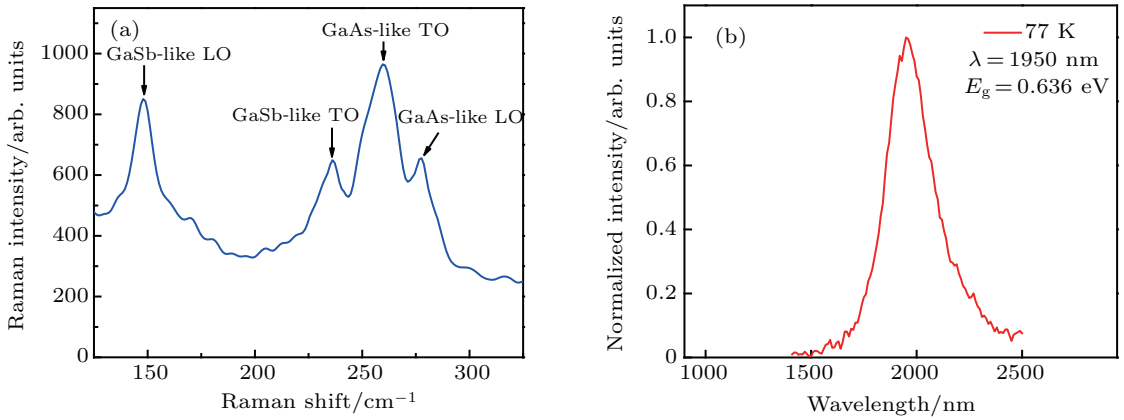


Fig. 3. (color online) (a) The Raman spectrum of the $Ga_{0.75}In_{0.25}As_{0.49}Sb_{0.51}$ nanowire. (b) The PL spectrum of $Ga_{0.75}In_{0.25}As_{0.49}Sb_{0.51}$ nanowires at 77 K.

In order to further characterize the microstructural properties of the as-grown $Ga_{0.75}In_{0.25}As_{0.49}Sb_{0.51}$ nanowires, we have performed the Raman and PL spectra measurements. As displayed in Fig. 3(a), the Raman spectrum excited with a continuous 632.8 nm laser was performed on a single nanowire. This spectrum shows a multi-mode phonon vibration behavior of GaInAsSb quaternary mixed crystal lattice. Distinct peaks in the broad spectrum ranging from 100 cm^{-1} to 300 cm^{-1} are

observed. The four phonon modes at 148 cm^{-1}, 236 cm^{-1}, 260 cm^{-1}, and 277 cm^{-1} are related to the GaSb-like longitudinal optical phonon (LO) modes,[31] the GaSb-like transverse optical phonon (TO) modes, the GaAs-like TO modes, and the GaAs-like LO modes, respectively.[32] This confirms that the achieved nanowires have good compositional homogeneity and high crystal quality. The PL spectrum of the nanowires at 77 K is shown in Fig. 3(b), which exhibits a single emission band with peak wavelength at 1950 nm, corresponding to the bandgap of ~ 0.636 eV. The bandgap can be calculated to be 0.615 eV through the equation[33]

$$E_g(x,y) = 0.359 + 0.48x - 0.78y - 0.398xy + 0.6x^2 + 0.596y^2 - 0.185x^2y + 0.054xy^2, \quad (1)$$

where x and y are 0.75 and 0.49 derived from $Ga_{0.75}In_{0.25}As_{0.49}Sb_{0.51}$. The difference between the bandgap values obtained from the PL spectrum and the calculation is less than 5%, indicating that the photoluminescence of the nanowires results from the band edge emission of the semiconductor alloy $Ga_{0.75}In_{0.25}As_{0.49}Sb_{0.51}$. The Raman and PL spectra are in good agreement with the structural composition described above, further demonstrating the high-quality of the $Ga_{0.75}In_{0.25}As_{0.49}Sb_{0.51}$ nanowires.

In order to investigate the photoresponse properties of the as-grown nanowires, PDs were constructed with the as-prepared single $Ga_{0.75}In_{0.25}As_{0.49}Sb_{0.51}$ nanowires. The single nanowire connected with the Cr/Au Schottky contact electrodes constitutes a typical M-S-M PD. Figure 4(a) provides the schematic image of the nanowire PDs. Figure 4(b) shows the *I*–*V* curves of a representative nanowire PD (see the inset) with a wire diameter of ~ 200 nm and a channel length of ~ 5.5 μm, measured in dark conditions and under the illumination of a monochromatic light beam with a wavelength of 980 nm at different light intensities. It can be seen that the electrical conductance of the device significantly increases when the light intensity rises from 10 mW/cm^2 to 260 mW/cm^2. Figure 4(c) plots the light intensity-dependent photocurrent with the working voltage at 1.0 V, which demonstrates an approximate linear dependency. The largest photoexcited current can reach 0.32 μA when the light intensity is raised to 260 mW/cm^2 (the dark current is about 150 nA obtained in Fig. 4(b)), showing that the photon-generated carriers are enhanced with the increased light intensity. The light intensity-dependent photoconductive gain demonstrates that the nanowire is a typical photon-dependent resistor, which is beneficial for applications in light power detection.

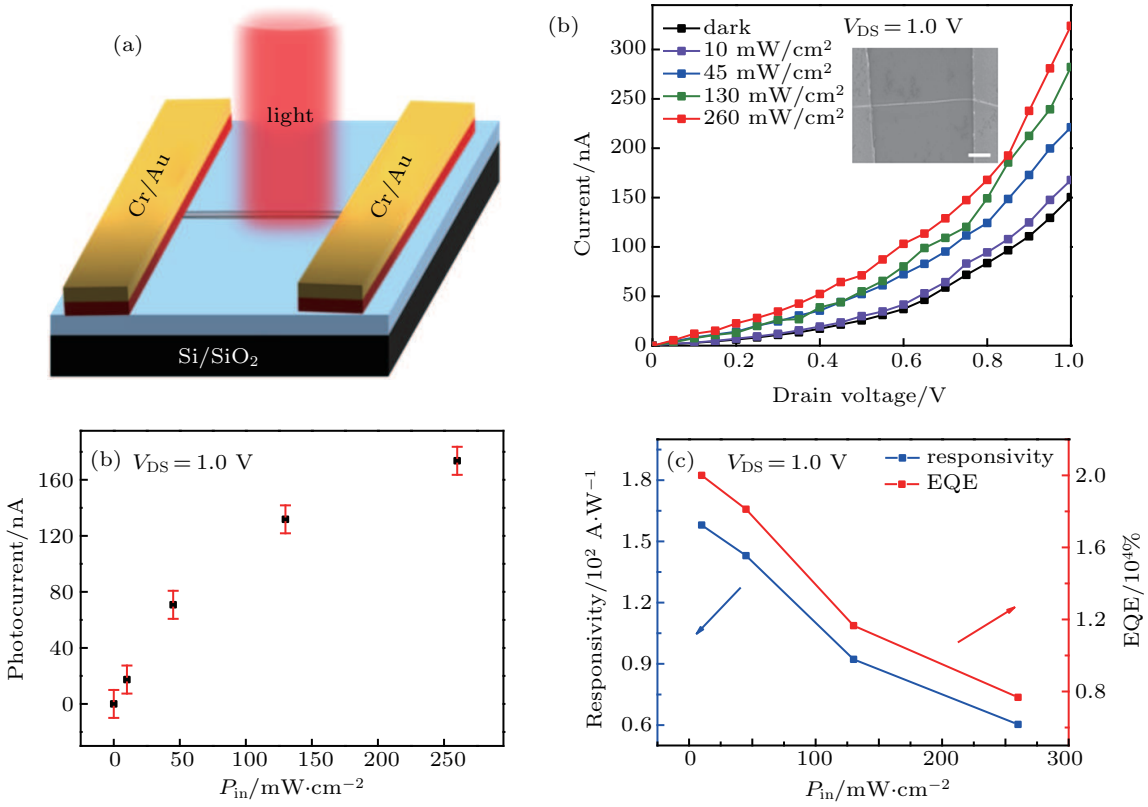


Fig. 4. (color online) (a) Schematic image of $Ga_{0.75}In_{0.25}As_{0.49}Sb_{0.51}$ nanowire PDs. (b) *I*–*V* curves of the device under 980 nm illumination at different light intensities. The inset shows the SEM image of a fabricated PD, scale bar: 1 μm. (c) Light intensity-dependence of the photocurrent at $V_{DS} = 1.0$ V. (d) Spectral responsivity *R* and EQE as functions of light intensity at $V_{DS} = 1.0$ V, respectively.

The spectral responsivity (R) and external quantum efficiency (EQE) are two critical parameters of a PD, which can be expressed as[34,35]

$$R = \frac{I_{\rm ph}}{PS}, \tag{2}$$

$$\mathrm{EQE} = R \times \frac{hc}{e\lambda}, \tag{3}$$

where $I_{\rm ph}$ is the photocurrent, P is the light intensity, S is the effective illuminated area, h is Plank's constant, c is the velocity of light, and λ is the incident light wavelength. The dependences of R and EQE on the light intensity under bias 1.0 V are shown in Fig. 4(d). When the incident light intensity is 10 mW/cm^2, the obtained R for this PD is 158 A/W and the EQE can reach to 2.0×10^4%, both of which are higher than those reported for GaInAsSb thin-film PDs[24] and are comparable with other previously reported single-nanostructured PDs.[36,37] The high R and EQE of the representative PD can be explained with two factors. Firstly, the large surface-to-volume ratio of the nanowires can easily induce the hole-trap states at the nanowire surface, and these trap states can somehow increase the photocurrent density effectively.[38,39] Secondly, the synthesized alloy nanowires with high crystalline quality can effectively facilitate the transport of carriers along the axis and cause a large photocurrent gain.[29,40]

4. Conclusion and perspectives

In summary, the $Ga_{0.75}In_{0.25}As_{0.49}Sb_{0.51}$ quaternary alloy nanowires have been successfully synthesized through a simple CVD method. Along the length of the nanowires, the composition distribution of the nanowires is uniform, and the nanowires are high quality zinc-blende single-crystal structured. These nanowires have strong light emission at 1950 nm, which is in accordance with their bandedge emission. The constructed PDs based on the alloy nanowires show a strong light response in the near-infrared region with high R (158 A/W) and EQE (2.0×10^4%). The synthesized quaternary alloy nanowires in this work will be a good candidate for construction of functional electronic and photoelectric devices.

References

[1] Feng J G, Jiang X Y, Yan X Y, Wu Y C, Su B, Fu H B, Yao J N and Jiang L 2017 *Adv. Mater.* **29** 1603652

[2] Zhang Q L, Wang S W, Liu X X, Chen T R, Li H F, Liang J W, Zheng W H Agarwal R, Lu W and Pan A L 2016 *Nano Energy* **30** 481

[3] Jevtics D, Hurtado A, Guilhabert B, McPhillimy J, Cantarella G, Gao Q, Tan H H, Jagadish C, Strain M J and Dawson M D 2017 *Nano Lett.* **17** 5990

[4] Kim K, Rho Y, Kim Y, Kim S H, Kim S G and Park C E 2016 *Adv. Mater.* **28** 3209

[5] Wang M X, Yue G H, Lin Y D, Wen X, Peng D L and Geng Z R 2013 *Nano-Micro Lett.* **5** 1

[6] Zhang W, Han W H, Zhao X S, Lv Q F, Ji X H, Yang T and Yang F H 2017 *Chin. Phys. B* **26** 088101

[7] Wu D, Tang X, Wang K and Li X 2016 *Opt. Express* **24** A1336

[8] Gong X, Tong M H, Xia Y J, Cai W Z, Moon J S, Cao Y, Yu G, Shieh C L, Nilsson B and Heeger A J 2009 *Science* **325** 1665

[9] Wang Q S, Li J, Lei Y, Wen Y, Wang Z X, Zhan X Y, Wang F, Wang F M, Huang Y, Xu K and He J 2016 *Adv. Mater.* **28** 3596

[10] Huang X, Yu Y Q, Jones T, Fan H, Wang L, Xia J, Wang Z J, Shao L D, Meng X M and Willinger M G 2016 *Adv. Mater.* **28** 7603

[11] Zhuang X J, Ning C Z and Pan A L 2012 *Adv. Mater.* **24** 13

[12] Song Z M, Zhao D X, Guo Z, Li B H, Zhang Z Z and Shen D Z 2012 *Acta Phys. Sin.* **61** 052901 (in Chinese)

[13] Kuo HC H, Wu J M, Lin S J and Chang W C 2013 *Nanoscale Res. Lett.* **8** 327

[14] Fang H H, Hu W D, Wang P, Guo N, Luo W J, Zheng D S, Gong F, Luo M, Tian H J, Zhang X T, Luo C, Wu X, Chen P P, Liao L, Pan A L, Chen X S and Lu W 2016 *Nano Lett.* **16** 6416

[15] Li L X, Pan D, Xue Y Z, Wang X L, Lin M L, Su D, Zhang Q L, Yu X Z, So H, Wei D H, Sun B Q, Tan P, Pan A L and Zhao J H 2017 *Nano Lett.* **17** 622

[16] Tan H, Fan C, Ma L, Zhang X H, Fan P, Yang Y K, Hu W, Zhou H, Zhuang X J, Zhu X L and Pan A L 2016 *Nano-Micro Lett.* **8** 29

[17] Ma L, Zhang X H, Li H L, Tan H, Yang Y K, Xu Y D, Hu W, Zhu X L, Zhuang X J and Pan A L 2015 *Semicond. Sci. Tech.* **30** 105033

[18] Ma L, Hu W, Zhang Q L, Ren P Y, Zhuang X J, Zhou H, Xu J Y, Li H L, Shan Z P, Wang X X, Liao L, Xu H Q and Pan A L 2014 *Nano Lett.* **14** 694

[19] Ren P Y, Zhu X L, Han J Y, Xu J Y, Ma L, Li H L, Zhuang X Z, Zhou H, Zhang Q L, Xia M G and Pan A 2014 *Nano-Micro Lett.* **6** 301

[20] Yang Y K, Yang T F, Li H L, Qi Z Y, Chen X L, Wu W Q, Hu X L, He P B, Jiang Y, Hu W, Zhang Q L, Zhuang X Z, Zhu X L and Pan A L 2016 *Chin. Phys. B* **25** 118106

[21] Xu Y D, Liu R P, Ma L, Li D, Yang Y K, Dai G Z and Wan Q 2017 *Appl. Phys. A* **123** 6

[22] Glisson T H, Hauser J R, Littlejohn M A and William C K 1978 *J. Electron. Mater.* **7** 1

[23] Ikyo A B, Marko I P, Hild K, Adams A R, Arafin S, Amann M C and Sweeney S J 2016 *Sci. Rep.* **6** 19595

[24] Bhagwat V, Xiao Y, Bhat I, Dutta P, Refaat T F, Abedin M N and Kumar V 2006 *J. Electron. Mater.* **35** 8

[25] Rakovics V, Tóth A L, Podör B, Frigeri C, Balázs J and Horváth Z E 2002 *Mater. Sci. Eng. B* **91** 83

[26] Cherng M J, Stringfellow G B, Kisker D W, Srivastava A K and Zyskind J L 1986 *Appl. Phys. Lett.* **48** 419

[27] Tsang W T, Chiu T H, Kisker D W and Ditzenberger J A 1985 *Appl. Phys. Lett.* **46** 283

[28] Li S W, Koike K, Schulze-Kraasch F and Kubalek E 2001 *J. Cryst. Growth* **223** 456

[29] Ren P Y, Hu W, Zhang Q L, Zhu X L, Zhuang X J, Ma L, Fan X P, Zhou H, Liao L, Duan X F and Pan A L 2014 *Adv. Mater.* **26** 7444

[30] Wagner R S and Ellis W C 1964 *Appl. Phys. Lett.* **4** 89

[31] Lugstein A, Schöndorfer C, Weil M, Tomastic C, Jauss A and Bertagnolli E 2007 *Nucl. Instrum. Methods Phys. Res., Sect. B* **255** 309

[32] Liang B L, Jiang C P, Xia G Q, Fan S P and Chu J H 2001 *J. Infrared Millim. Waves* **20** 315

[33] Li S W, Jin Y X, Zhou T M, Zhang B L, Ning Y Q, Jiang H, Yuan G, Zhang X Y and Yuan J S 1995 *J. Cryst. Growth* **156** 39

[34] Miao J S, Hu W D, Guo N, Lu Z Y, Zou X M, Liao L, Shi S X, Chen P P, Fan Z Y, Ho J C, Li T X, Chen X S and Lu W 2014 *ACS Nano* **8** 3628

[35] Guo P F, Xu J Y, Gong K, Shen X, Lu Y, Qiu Y, Xu J Q, Zou Z J, Wang C L, Yan H L, Luo Y S, Pan A L, Zhang H, Ho J C and Yu K M 2016 *ACS Nano* **10** 8474

[36] Chen X L, Li H L, Qi Z Y, Yang T F, Yang Y K, Hu X L, Zhang X H, Zhu X L, Zhuang X J, Hu W and Pan A L 2016 *Nanotechnology* **27** 505602

[37] Ali Z, Mirza M, Cao C B, Butt F K, Tanveer M, Tahir M, Aslam I, Idrees F and Safdar M 2014 *ACS Appl. Mater. Interfaces* **6** 9550

[38] Xie X M and Shen G Z 2015 *Nanoscale* **7** 5046

[39] Xu W, Chin A, Ye L, Ning C Z and Yu H B 2012 *J. Appl. Phys.* **111** 104515

[40] Guo N, Hu W D, Liao L, Yip S P, Ho J C, Miao J S, Zhang Z, Zou J, Jiang T, Wu S W, Chen X S and Lu W 2014 *Adv. Mater.* **26** 8203